Journal of
Mechanics of
Materials and Structures

ON THE CAUSALITY OF THE RAYLEIGH WAVE

Barış Erbaş and Onur Şahin

Volume 11, No. 4 July 2016

msp

JOURNAL OF MECHANICS OF MATERIALS AND STRUCTURES
Vol. 11, No. 4, 2016
dx.doi.org/10.2140/jomms.2016.11.449

ON THE CAUSALITY OF THE RAYLEIGH WAVE

BARIŞ ERBAŞ AND ONUR ŞAHIN

An explicit hyperbolic-elliptic formulation for surface Rayleigh waves is analysed with an emphasis on the causality of obtained results. As an example, a 3D moving load problem for a distributed vertical load is considered. A simple approximate solution is derived for a near-resonant regime, and the related point load solution is recast as a limiting case. It is shown that causality is characteristic only for the longitudinal wave potential along the surface, where it is governed by a hyperbolic equation modelling the small dilatation disturbances propagating at the Rayleigh wave speed.

1. Introduction

Propagation of surface waves has been investigated in numerous papers since the original contribution of Rayleigh [1885]. In his well-known work, Chadwick [1976] presented a general formulation of the Rayleigh wave field in terms of a single harmonic function. His results have been recently generalised to 3D by Kiselev and Parker [2010]. Parker [2012] later generalised their results for evanescent Schölte waves with an arbitrary profile. Surface waves in layered structures [Kiselev and Rogerson 2009; Kiselev et al. 2007] have also attracted considerable attention. Among other contributions, we note the approach of Rousseau and Maugin [2011] associating the quasiparticles with the Rayleigh wave, along with papers developing the mathematical theory of surface waves in anisotropic media, e.g., [Achenbach 1998; Prikazchikov 2013; Parker 2013].

The issue of causality of the Rayleigh wave does not usually arise in linear elasticity governed by hyperbolic equations with the characteristics corresponding to longitudinal and transverse wave speeds; see, e.g., [Achenbach 1973; Poruchikov 1993]. This is only a feature of the specialised hyperbolic-elliptic model oriented to the Rayleigh wave and neglecting bulk waves [Kaplunov et al. 2006; Erbaş et al. 2013; Kaplunov and Prikazchikov 2013]. The advantages of this model are illustrated by investigation of the near-resonant regimes of moving loads on an elastic half-space [Kaplunov et al. 2010; 2013; Erbaş et al. 2014].

In the case of a vertical load, the implementation of the aforementioned model begins with solving a scalar hyperbolic equation for the longitudinal wave potential on the surface. The characteristics of this equation are associated with the Rayleigh wave speed. Then the variation of the longitudinal potential over the interior is found from a Dirichlet problem for a pseudostatic elliptic equation with the boundary condition coming from the solution of the wave equation on the surface. Finally, the transverse wave potential is determined. In particular, in the plane-strain setup, it is recovered as the harmonic conjugate of the longitudinal wave potential; see also [Chadwick 1976].

It is obvious that we may only expect causality of the longitudinal wave potential along the surface, where it is governed by a hyperbolic equation. The causality concept is not applicable to the transverse

Keywords: moving load, causality, Rayleigh wave, hyperbolic-elliptic model.

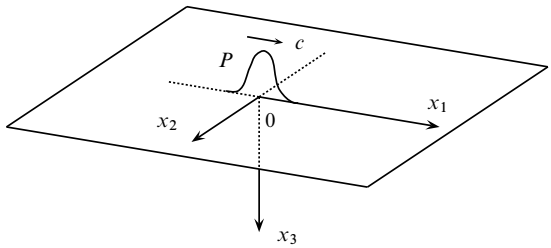

Figure 1. Distributed load moving along the x_1 axis.

wave potential and the longitudinal wave potential over the interior, where both of them satisfy elliptic equations. Fortunately, this only means that the considered surface wave formulation is valid only behind bulk wave fronts. However, the presence of bulk waves ignored within this formulation may also hypothetically result in formally noncausal solutions of the wave equation on the surface; see the discussion of the Mach cones associated with a super-Rayleigh moving load in [Erbaş et al. 2014].

In this paper, we revisit the 3D steady-state moving load problem for an elastic half-space studied earlier in [Kaplunov et al. 2013], with a special focus on the causality of the Rayleigh wave, including analysis of the associated Mach cones. In contrast to [Erbaş et al. 2014] dealing with a point force, we are mainly concerned with the case a distributed load, which is seemingly more relevant to modern engineering applications, motivated by modelling of high-speed trains; see, e.g., [Cao et al. 2012; Galvín and Domínguez 2007; El Kacimi et al. 2013; Gupta et al. 2010; Agostinacchio et al. 2013; Dieterman and Metrikine 1997; Celebi 2006].

The paper is organised as follows. In Section 2, we formulate the problem in terms of the aforementioned hyperbolic-elliptic model. In Section 3, the super-Rayleigh solution on the surface is analysed, with the causality concept embedded. Then the solution over the interior is constructed via the Poisson formula, and the components of the transverse wave potentials are determined with the help of the relevant differential relations on the surface. In Section 4, the steady-state solution for a *distributed load* over the interior of the half-space is obtained. Finally, in Section 5, comparisons of solutions for point and distributed forces are illustrated numerically.

2. Statement of the problem

We consider the dynamic response of a 3D elastic isotropic half-space ($-\infty < x_1, x_2 < \infty$, $0 \le x_3 < \infty$) under the influence of a vertical load of magnitude P distributed along the x_1 axis and moving along its positive direction on the surface $x_3 = 0$ of the half-space at a constant speed c; see Figure 1.

In this paper, we employ a hyperbolic-elliptic approximate model for the surface wave field [Kaplunov et al. 2006; Erbaş et al. 2013]. Within the framework of this model, the Lamé potentials φ and ψ_i, $i = 1, 2$, satisfy the pseudostatic elliptic equations over the interior

$$\frac{\partial^2 \varphi}{\partial x_3^2} + k_1^2 \Delta_2 \varphi = 0, \qquad \frac{\partial^2 \psi_i}{\partial x_3^2} + k_2^2 \Delta_2 \psi_i = 0, \quad i = 1, 2, \tag{2-1}$$

where $\Delta_2 = \partial^2/\partial x_1^2 + \partial^2/\partial x_2^2$ is a 2D Laplacian, $k_i^2 = 1 - c_R^2/c_i^2$, $i = 1, 2$, and c_1, c_2 and c_R are the longitudinal, transverse and Rayleigh wave speeds, respectively. The components of the displacement

vector may be written in terms of the Lamé potentials as

$$u_1 = \frac{\partial\varphi}{\partial x_1} - \frac{\partial\psi_1}{\partial x_3}, \qquad u_2 = \frac{\partial\varphi}{\partial x_2} - \frac{\partial\psi_2}{\partial x_3}, \qquad u_3 = \frac{\partial\varphi}{\partial x_3} + \frac{\partial\psi_1}{\partial x_1} + \frac{\partial\psi_2}{\partial x_2}; \tag{2-2}$$

for more details, see [Kaplunov and Prikazchikov 2013]. The boundary conditions on the surface $x_3 = 0$ include the hyperbolic equation

$$\Delta_2\varphi - \frac{1}{c_R^2}\frac{\partial^2\varphi}{\partial t^2} = AP\frac{a}{\pi[(x_1 - ct)^2 + a^2]}\delta(x_2), \tag{2-3}$$

together with the relations between the potentials

$$\frac{\partial\varphi}{\partial x_i} = \frac{2}{1+k_2^2}\frac{\partial\psi_i}{\partial x_3}, \quad i = 1, 2. \tag{2-4}$$

In (2-3), A is a constant depending on the material properties of a half-space given by

$$A = \frac{k_1k_2(1+k_2^2)}{2\mu[k_2(1-k_1^2) + k_1(1-k_2^2) - k_1k_2(1-k_2^4)]}. \tag{2-5}$$

Throughout the paper, we are mainly concerned with the steady-state regime in the moving frame related to the coordinate $\lambda = x_1 - ct$. Rewriting (2-3) in the new coordinates, we get for the sub-Rayleigh ($c < c_R$) and super-Rayleigh ($c > c_R$) cases, respectively,

$$\frac{\partial^2\varphi}{\partial x_2^2} + \varepsilon^2\frac{\partial^2\varphi}{\partial\lambda^2} = AP\frac{a}{\pi[\lambda^2 + a^2]}\delta(x_2), \tag{2-6}$$

$$\frac{\partial^2\varphi}{\partial x_2^2} - \varepsilon^2\frac{\partial^2\varphi}{\partial\lambda^2} = AP\frac{a}{\pi[\lambda^2 + a^2]}\delta(x_2), \tag{2-7}$$

where

$$\varepsilon = \left|1 - \frac{c^2}{c_R^2}\right|^{1/2}. \tag{2-8}$$

The adopted approximate formulation is valid when the load speed is close to the Rayleigh wave speed, i.e., when $\varepsilon \ll 1$, which enables investigation of the near-resonant response dominated by the Rayleigh wave contribution [Kaplunov et al. 2010; 2013]. Introducing the scaled variables

$$\xi_1 = \frac{\lambda}{\varepsilon}, \qquad \xi_2 = x_2, \qquad \xi_3 = \frac{x_3}{\varepsilon}, \tag{2-9}$$

the elliptic equations (2-1) become

$$\begin{gathered}\frac{\partial^2\varphi}{\partial\xi_3^2} + k_1^2\frac{\partial^2\varphi}{\partial\xi_1^2} + \varepsilon^2k_1^2\frac{\partial^2\varphi}{\partial\xi_2^2} = 0,\\ \frac{\partial^2\psi_i}{\partial\xi_3^2} + k_2^2\frac{\partial^2\psi_i}{\partial\xi_1^2} + \varepsilon^2k_2^2\frac{\partial^2\psi_i}{\partial\xi_2^2} = 0, \quad i = 1, 2,\end{gathered} \tag{2-10}$$

along with boundary conditions (2-6) and (2-7) on the surface $\xi_3 = 0$ rewritten as

$$\frac{\partial^2\varphi}{\partial\xi_2^2} + \frac{\partial^2\varphi}{\partial\xi_1^2} = AP\frac{a}{\pi[\varepsilon^2\xi_1^2 + a^2]}\delta(\xi_2), \tag{2-11}$$

$$\frac{\partial^2\varphi}{\partial\xi_2^2} - \frac{\partial^2\varphi}{\partial\xi_1^2} = AP\frac{a}{\pi[\varepsilon^2\xi_1^2 + a^2]}\delta(\xi_2). \tag{2-12}$$

The relations (2-4) for the potentials φ, ψ_1 and ψ_2 now take the form

$$\frac{\partial\varphi}{\partial\xi_1} = \frac{2}{1+k_2^2}\frac{\partial\psi_1}{\partial\xi_3}, \qquad \frac{\partial\varphi}{\partial\xi_2} = \frac{2}{\varepsilon(1+k_2^2)}\frac{\partial\psi_2}{\partial\xi_3}. \tag{2-13}$$

3. Revisit of the moving point force problem

Before considering the problem (2-10)–(2-13) for a distributed load, let us discuss the solution for a point force for the super-Rayleigh regime ($c > c_R$) earlier treated in [Kaplunov et al. 2013]. In the limit $a \to 0$, the hyperbolic equation on the surface (2-3) becomes

$$\Delta_2\varphi - \frac{1}{c_R^2}\frac{\partial^2\varphi}{\partial t^2} = AP\delta(x_1 - ct)\delta(x_2). \tag{3-1}$$

The fundamental solution of the 2D wave equation is given by

$$\mathcal{F}(x_1, x_2, t) = -\frac{c_R H\left(c_R t - \sqrt{x_1^2 + x_2^2}\right)}{2\pi\sqrt{c_R^2 t^2 - x_1^2 - x_2^2}} \tag{3-2}$$

[Zauderer 2006], where $H(x)$ is the Heaviside function. As might be expected, it is causal in the variables x_1, x_2 and t. Then the solution of (3-1) may be expressed as a convolution, i.e.,

$$\begin{aligned}\varphi(x_1, x_2, 0, t) &= \int_0^t \mathcal{F}(x_1 - ct, x_2, t - \tau)\, d\tau \\ &= -\frac{APc_R}{2\pi}\int_0^t \frac{H\left(c_R(t-\tau) - \sqrt{(x_1 - c\tau)^2 + x_2^2}\right)}{\sqrt{c_R^2(t-\tau)^2 - (x_1 - c\tau)^2 - x_2^2}}\, d\tau,\end{aligned} \tag{3-3}$$

or in the form

$$\varphi(\lambda, x_2, 0) = -\frac{APc_R}{2\pi}\int_0^t \frac{H\left(c_R s - \sqrt{(\lambda + cs)^2 + x_2^2}\right)}{\sqrt{(c_R^2 - c^2)s^2 - 2sc\lambda - \lambda^2 - x_2^2}}\, ds, \tag{3-4}$$

where $s = t - \tau$. The argument of the Heaviside function in the numerator of (3-4) is positive when $\lambda < 0$ in the considered super-Rayleigh case and $s_1 \le s \le s_2$, where

$$s_1 = n + \sqrt{n^2 - m}, \qquad s_2 = n - \sqrt{n^2 - m}, \tag{3-5}$$

with

$$n = -\frac{\lambda c}{c^2 - c_R^2}, \qquad m = \frac{\lambda^2 + x_2^2}{(c^2 - c_R^2)^2}. \tag{3-6}$$

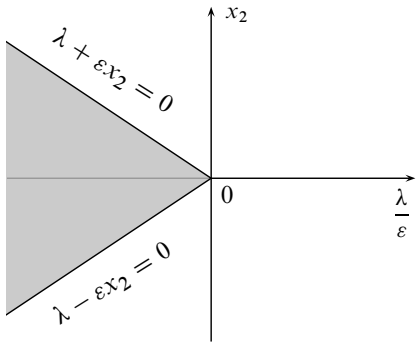

Figure 2. Mach cone.

As $t \to \infty$,

$$\varphi(\lambda, x_2, 0) = -\frac{APc_R}{2\pi} \int_{s_1}^{s_2} \frac{1}{\sqrt{(c_R^2 - c^2)s^2 - 2sc\lambda - \lambda^2 - x_2^2}}\, ds = -\frac{AP}{2\varepsilon}. \tag{3-7}$$

We note that the roots s_1 and s_2 are real, provided that $n^2 - m \geq 0$; hence, $\varepsilon^2 x_2^2 - \lambda^2 \leq 0$. Therefore, since $\lambda < 0$,

$$\varphi(\lambda, x_2, 0) = \frac{AP}{2\varepsilon}\left[H\left(x_2 - \frac{\lambda}{\varepsilon}\right) - H\left(x_2 + \frac{\lambda}{\varepsilon}\right)\right] H(-\lambda). \tag{3-8}$$

The obtained solution (3-8) does not violate the causality concept and predicts the Mach cone shown in Figure 2. At the same time, we could immediately arrive at the same result by introducing the moving coordinate λ into (3-1) to get

$$\frac{\partial^2 \varphi}{\partial x_2^2} - \varepsilon^2 \frac{\partial^2 \varphi}{\partial \lambda^2} = A\delta(\lambda)\delta(x_2). \tag{3-9}$$

It is interesting that making use of the conventional fundamental noncausal solution in the variables λ and x_2 in (3-9) results in (3-8) without the factor $H(-\lambda)$ enabling the causality [Kaplunov et al. 2013]. Similar to [Kaplunov et al. 2013], the potential φ may now be recovered over the interior, $x_3 > 0$, through the Poisson formula [Courant and Hilbert 1962], resulting in

$$\varphi(\lambda, x_2, x_3) = \frac{AP}{2\pi\varepsilon} k_1 \eta_3 \int_{-\infty}^{0} \frac{H(x_2 - \eta/\varepsilon) - H(x_2 + \eta/\varepsilon)}{(\eta - \lambda)^2 + k_1 x_3^2}\, d\eta = \frac{AP}{2\pi\varepsilon} \cot^{-1}\left(\frac{\lambda + \varepsilon|x_2|}{k_1 x_3}\right). \tag{3-10}$$

It is now a simple matter to get the potentials ψ_1 and ψ_2 using the relations (2-4). The result is

$$\psi_1(\lambda, x_2, x_3) = -\frac{APk_1(1 + k_2^2)}{8\pi\varepsilon k_2^2} \ln(k_2^2 x_3^2 + (\lambda + \varepsilon|x_2|)^2), \tag{3-11}$$

$$\psi_2(\lambda, x_2, x_3) = -\frac{APk_1(1 + k_2^2)\,\mathrm{sgn}(x_2)}{8\pi k_2^2} \ln(k_2^2 x_3^2 + (\lambda + \varepsilon|x_2|)^2). \tag{3-12}$$

In what follows, we illustrate the behaviour of potentials for different values of the depth x_3 — specif-

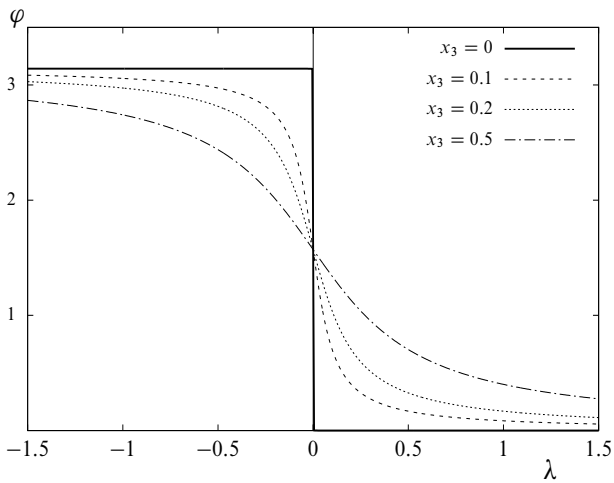

Figure 3. Potential φ versus λ at $x_2 = 0$.

ically, in Figure 3 we consider $x_3 = 0$, 0.1, 0.2 and 0.5. It is seen that on the surface $x_3 = 0$ the causality principle holds true, that is, there is no contribution of the longitudinal wave potential φ appearing in front of the load. However, as the depth increases ($x_3 > 0$), it is observed that in the interior of the half-space there appear some disturbances in front of the moving load. Figure 4 illustrates variation of the potentials ψ_1 and ψ_2 for different depths. It is clear from Figure 4 and also from (3-11) and (3-12) that the causality principle is not applicable to potentials ψ_1 and ψ_2, i.e., they may be treated as nonwave potentials.

Thus, within the framework of the approximate formulation of the Rayleigh wave, the causality principle is only valid on the surface and only for the longitudinal wave potential φ.

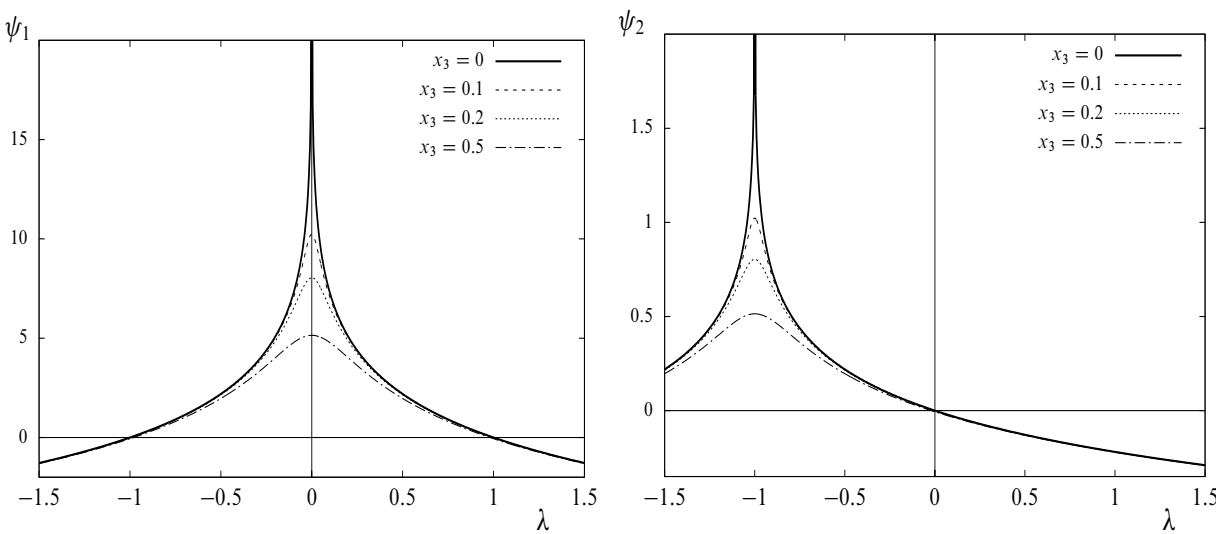

Figure 4. Potentials ψ_1 and ψ_2 versus λ at $x_2 = 0$ and $x_2 = 1$, respectively.

4. Solution for distributed force

We may now derive the steady-state solution of (2-10)–(2-13) employing the adopted hyperbolic-elliptic model. Consider first the super-Rayleigh regime. At leading order, elliptic equations (2-10) give

$$\frac{\partial^2\varphi}{\partial\xi_3^2}+k_1^2\frac{\partial^2\varphi}{\partial\xi_1^2}=0,\qquad \frac{\partial^2\psi_i}{\partial\xi_3^2}+k_2^2\frac{\partial^2\psi_i}{\partial\xi_1^2}=0,\quad i=1,2, \tag{4-1}$$

which should be solved together with the hyperbolic equation (2-7) and relations (2-4). Using the fundamental solution of the wave operator

$$F(\xi_1,\xi_2)=\tfrac{1}{2}[H(\xi_2-\xi_1)-H(\xi_2+\xi_1)], \tag{4-2}$$

for $\xi_1<0$, from the causality, the longitudinal wave potential on the surface may easily be obtained in the form

$$\varphi(\xi_1,\xi_2,0)=\frac{AP}{2\pi\varepsilon}\left[\frac{\pi}{2}-\tan^{-1}(\alpha(\xi_1+|\xi_2|))\right], \tag{4-3}$$

where the notation $\alpha=\varepsilon/a$ is introduced. The sought-after solution for the Dirichlet problem for elliptic equation (4-1) may be written using the 2D Poisson integral formula giving

$$\begin{aligned}\varphi(\xi_1,\xi_2,\xi_3)&=\frac{AP}{2\pi^2\varepsilon}k_1\xi_3\left\{\frac{\pi}{2}\int_{-\infty}^{\infty}\frac{1}{(\eta-\xi_1)^2+k_1^2\xi_3^2}\,d\eta-\int_{-\infty}^{\infty}\frac{\tan^{-1}(\alpha(\eta+|\xi_2|))}{(\eta-\xi_1)^2+k_1^2\xi_3^2}\,d\eta\right\}\\&=\frac{AP}{2\pi\varepsilon}\cot^{-1}\left(\frac{\alpha(\xi_1+|\xi_2|)}{1+\alpha k_1\xi_3}\right).\end{aligned} \tag{4-4}$$

In order to obtain the transverse wave potentials ψ_1 and ψ_2, we employ relations (2-13). Differentiation of (4-4) gives

$$\frac{\partial\varphi(\xi_1,\xi_2,\xi_3)}{\partial\xi_1}=-\frac{AP}{2\pi a}\frac{1+\alpha k_1\xi_3}{(1+\alpha k_1\xi_3)^2+\alpha^2(\xi_1+|\xi_2|)^2}. \tag{4-5}$$

Taking into account $(4\text{-}1)_2$ and $(2\text{-}13)_1$, we get

$$\frac{\partial\psi_1(\xi_1,\xi_2,\xi_3)}{\partial\xi_3}=-\frac{AP(1+k_2^2)}{4\pi a}\frac{1+\alpha k_2\xi_3}{(1+\alpha k_2\xi_3)^2+\alpha^2(\xi_1+|\xi_2|)^2}; \tag{4-6}$$

hence,

$$\psi_1(\xi_1,\xi_2,\xi_3)=-\frac{AP(1+k_2^2)}{8\pi\varepsilon k_2}\ln((1+\alpha k_2\xi_3)^2+\alpha^2(\xi_1+|\xi_2|)^2). \tag{4-7}$$

Using $(2\text{-}13)_2$ and following the same procedure as above, we obtain

$$\psi_2(\xi_1,\xi_2,\xi_3)=-\frac{AP\,\mathrm{sgn}(\xi_2)(1+k_2^2)}{8\pi k_2}\ln((1+\alpha k_2\xi_3)^2+\alpha^2(\xi_1+|\xi_2|)^2). \tag{4-8}$$

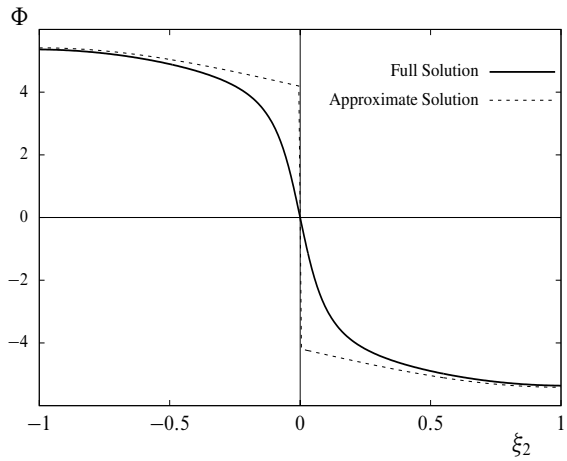

Figure 5. Derivatives of super-Rayleigh full and approximate solutions, for $\nu = 0.25$, $a = 0.1$, $\varepsilon = 0.1$, $\xi_1 = -1$ and $\xi_3 = 1$.

Rewriting (2-2) in terms of scaled variables (2-9) and using the results (4-4), (4-7) and (4-8), we get for the displacement components

$$u_1 = \frac{\alpha}{\varepsilon^2}\frac{AP}{2\pi}\left[\frac{1+k_2^2}{2}\frac{1+\alpha k_2\xi_3}{(1+\alpha k_2\xi_3)^2+\alpha^2(\xi_1+|\xi_2|)^2} - \frac{1+\alpha k_1\xi_3}{(1+\alpha k_1\xi_3)^2+\alpha^2(\xi_1+|\xi_2|)^2}\right], \tag{4-9}$$

$$u_2 = \frac{AP\alpha\,\mathrm{sgn}(\xi_2)}{2\pi\varepsilon}\left[\frac{1+k_2^2}{2}\frac{1+\alpha k_2\xi_3}{(1+\alpha k_2\xi_3)^2+\alpha^2(\xi_1+|\xi_2|)^2} - -\frac{1+\alpha k_1\xi_3}{(1+\alpha k_1\xi_3)^2+\alpha^2(\xi_1+|\xi_2|)^2}\right], \tag{4-10}$$

$$\begin{aligned} u_3 = &-\frac{AP\alpha^2(1+k_2^2)}{4\pi k_2}\frac{\xi_1+|\xi_2|}{(1+\alpha k_2\xi_3)^2+\alpha^2(\xi_1+|\xi_2|)^2} \\ &-\frac{AP\alpha^2}{2\pi\varepsilon^2}\left[\frac{(1+k_2^2)}{2k_2}\frac{\xi_1+|\xi_2|}{(1+\alpha k_2\xi_3)^2+\alpha^2(\xi_1+|\xi_2|)^2} - k_1\frac{\xi_1+|\xi_2|}{(1+\alpha k_1\xi_3)^2+\alpha^2(\xi_1+|\xi_2|)^2}\right]. \end{aligned} \tag{4-11}$$

We remark that keeping the $O(\varepsilon^2)$ terms in the elliptic equations (4-1), the full solution for the potential φ may be obtained via Poisson's formula for a half-space, giving

$$\varphi(\xi_1,\xi_2,\xi_3) = \frac{AP\xi_3}{4\pi^2\varepsilon}\int_{-\infty}^{\infty}\int_{-\infty}^{\infty}\frac{\cot^{-1}(\alpha k_1(\eta_1+\varepsilon|\eta_2|))}{[(\eta_1-\xi_1/k_1)^2+(\eta_2-\xi_2/(\varepsilon k_1))^2+\xi_3^2]^{3/2}}\,d\eta_1\,d\eta_2. \tag{4-12}$$

We may now compare the approximate solution (4-4) with its full counterpart (4-12) for the longitudinal wave potential φ. We compare the normalised derivative $\Phi = (2\pi/AP)\partial\varphi/\partial\xi_2$ in Figure 5.

Let us now present the results for the sub-Rayleigh regime ($c < c_R$). The solution of (2-11) on the surface $x_3 = 0$ may be written as

$$\varphi(\xi_1,\xi_2,0) = \frac{AP}{4\pi\varepsilon}\ln(\xi_1^2+(\alpha^{-1}+|\xi_2|)^2). \tag{4-13}$$

The approximate solution over the interior follows, again, from the 2D Poisson formula giving

$$\varphi(\xi_1,\xi_2,\xi_3) = \frac{AP}{4\pi\varepsilon}\ln(\xi_1^2+(|\xi_2|+k_1\xi_3+\alpha^{-1})^2). \tag{4-14}$$

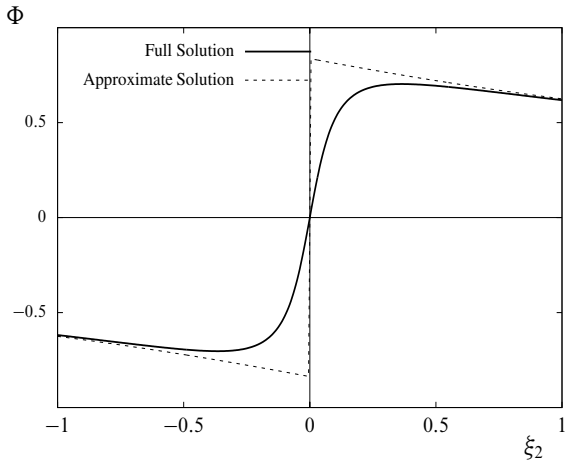

Figure 6. Derivatives of sub-Rayleigh full and approximate solutions for $a = 0.1$, $\varepsilon = 0.1$, $\xi_1 = -1$ and $\xi_3 = 1$.

The full solution of the sub-Rayleigh case may be expressed in an integral form as

$$\varphi(\xi_1, \xi_2, \xi_3) = \frac{AP\xi_3}{8\pi^2\varepsilon} \int_{-\infty}^{\infty}\int_{-\infty}^{\infty} \frac{\ln((\eta_1/\varepsilon)^2 + ((\varepsilon\alpha k_1)^{-1} + |\eta_2|)^2)}{[(\eta_1 - \xi_1/k_1)^2 + (\eta_2 - \xi_2/(\varepsilon k_1))^2 + \xi_3^2]^{3/2}}\, d\eta_1\, d\eta_2. \tag{4-15}$$

The numerical comparison of the normalised derivative of the full and approximate solutions, $\Phi = (4\pi\varepsilon/AP)\partial\varphi/\partial\xi_2$, is presented in Figure 6.

Following the procedure presented in detail for the super-Rayleigh case, potentials ψ_1 and ψ_2 are found to be

$$\psi_1(\xi_1, \xi_2, \xi_3) = \frac{AP(1+k_2^2)}{4\pi\varepsilon k_2} \tan^{-1}\left(\frac{|\xi_2| + k_2\xi_3 + \alpha^{-1}}{\xi_1}\right), \tag{4-16}$$

$$\psi_2(\xi_1, \xi_2, \xi_3) = \frac{AP\,\mathrm{sgn}(\xi_2)(1+k_2^2)}{8\pi k_2} \ln(\xi_1^2 + (|\xi_2| + k_2\xi_3 + \alpha^{-1})^2). \tag{4-17}$$

The resulting displacement components are

$$u_1 = \frac{1}{\varepsilon^2}\frac{AP}{2\pi}\left[\frac{\xi_1}{\xi_1^2 + (|\xi_2| + k_1\xi_3 + \alpha^{-1})^2} - \frac{1+k_2^2}{2}\frac{\xi_1}{\xi_1^2 + (|\xi_2| + k_2\xi_3 + \alpha^{-1})^2}\right], \tag{4-18}$$

$$u_2 = \frac{1}{\varepsilon}\frac{AP\,\mathrm{sgn}(\xi_2)}{2\pi}\left[\frac{|\xi_2| + k_1\xi_3 + \alpha^{-1}}{\xi_1^2 + (|\xi_2| + k_1\xi_3 + \alpha^{-1})^2} - \frac{1+k_2^2}{2}\frac{|\xi_2| + k_2\xi_3 + \alpha^{-1}}{\xi_1^2 + (|\xi_2| + k_2\xi_3 + \alpha^{-1})^2}\right], \tag{4-19}$$

$$u_3 = \frac{AP(1+k_2^2)}{4\pi k_2}\frac{|\xi_2| + k_2\xi_3 + \alpha^{-1}}{\xi_1^2 + (|\xi_2| + k_2\xi_3 + \alpha^{-1})^2} + \frac{1}{\varepsilon^2}\frac{AP}{2\pi}\left[k_1\frac{|\xi_2| + k_1\xi_3 + \alpha^{-1}}{\xi_1^2 + (|\xi_2| + k_1\xi_3 + \alpha^{-1})^2} - \frac{1+k_2^2}{2k_2}\frac{|\xi_2| + k_2\xi_3 + \alpha^{-1}}{\xi_1^2 + (|\xi_2| + k_2\xi_3 + \alpha^{-1})^2}\right]. \tag{4-20}$$

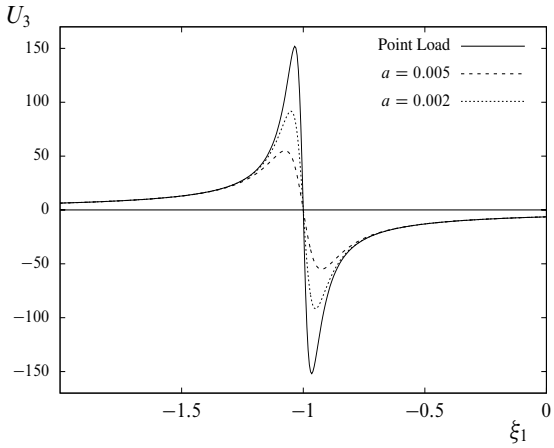

Figure 7. Super-Rayleigh vertical displacement versus ξ_1 for $a = 0.005$, $a = 0.002$ and the point load ($a = 0$).

5. Numerical comparison of solutions for point and distributed forces

In this section, we illustrate numerically the comparisons of the results for distributed load against those for point load discussed in [Kaplunov et al. 2013]. To this end, we set Poisson's ratio to $\nu = 0.25$ corresponding to the value $c_R = 0.9194c_2$. In the present problem, the load exhibits a gaussian-like profile, and as the parameter a approaches zero, the profile becomes a delta function moving along the x_1 axis. It is reasonable to expect, as a gets smaller, a considerable agreement between the displacements of both problems. We employ the same normalisation for the displacements presented in Section 5 of [Kaplunov et al. 2013], namely

$$U_i(\xi_1, \xi_2, \xi_3) = \frac{2\pi}{AP} u_i(\xi_1, \xi_2, \xi_3).$$

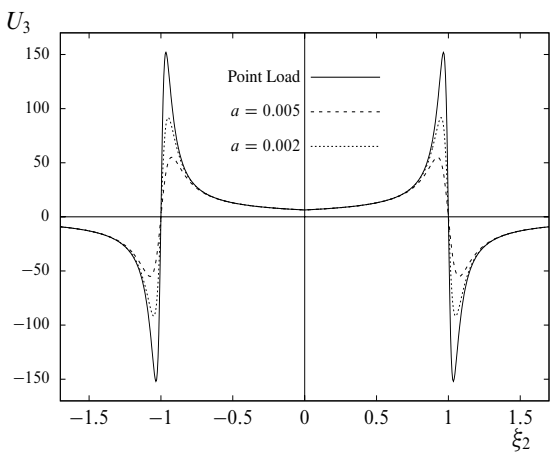

Figure 8. Super-Rayleigh vertical displacement versus ξ_2 for $a = 0.005$, $a = 0.002$ and the point load ($a = 0$).

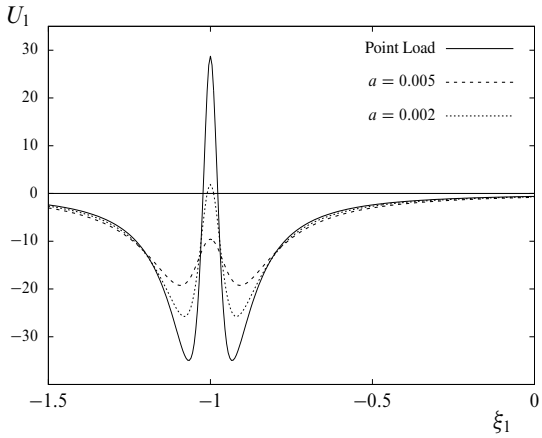

Figure 9. Super-Rayleigh horizontal displacement versus ξ_1 for $a = 0.005$, $a = 0.002$ and the point load ($a = 0$).

We first consider the super-Rayleigh case for which the load speed is taken as $c = 0.924c_2$ corresponding to $\varepsilon = 0.1$. Figure 7 displays comparisons of vertical displacements U_3 plotted against the moving coordinate ξ_1, with the depth being $\xi_3 = 0.1$. As expected, the singular behaviour under the point load corresponding to the coordinate $\xi_1 = -1$ is smoothed out by the distributed load, and it is clear that in the limit as $a \to 0$ we recover the solution for the point load problem. Figure 8 demonstrates the variation of the vertical displacement U_3 against the other horizontal variable ξ_2. Here, we take $\xi_1 = -1$ at depth $\xi_3 = 0.1$. A similar surface discontinuity is also evident here, which is again flattened for large values of a. Figure 9 presents a cross-section of displacement U_1. We observe that the delta-like profile near the singularity for the point load has been smoothed by the inclusion of the parameter a. Finally, numerical illustration for the sub-Rayleigh case is presented in Figure 10, which shows variation of the vertical displacement U_3 along the horizontal variable ξ_2. In the sub-Rayleigh case, the speed of the load is taken as $c = 0.9148c_2$, corresponding again to $\varepsilon = 0.1$.

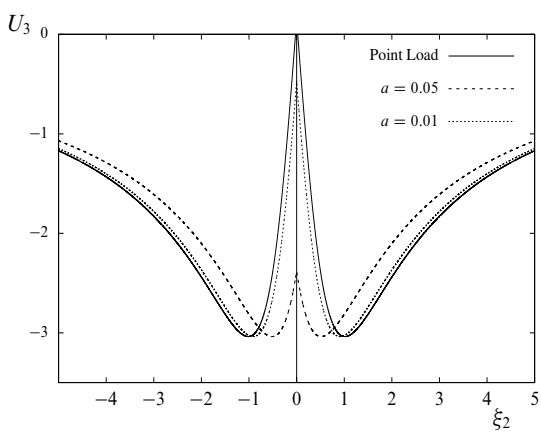

Figure 10. Sub-Rayleigh vertical displacement versus ξ_2 for $a = 0.05$, $a = 0.01$ and the point load ($a = 0$).

6. Concluding remarks

In this paper, a 3D problem for a distributional load of a gaussian-like profile moving along the surface of an elastic half-space is investigated. The hyperbolic-elliptic model in [Kaplunov and Prikazchikov 2013; Kaplunov et al. 2013] is specialised to tackle near-resonant behaviour ignoring the effect of longitudinal and transverse bulk waves. The presence of a small parameter expressing the proximity of the load speed to the Rayleigh wave speed enables us to reduce the 3D elliptic problems for the interior to 2D ones for the vertical cross-section along the load trajectory.

Various aspects of the Rayleigh wave causality are addressed. In contrast to the consideration in [Kaplunov et al. 2013], the steady-state location of the Mach cones, characteristic of the super-Rayleigh regime, is evaluated at a large time limit of the associated transient solution. Noncausality of the transverse wave potential, as well as the longitudinal wave potential over the interior, is due to the approximate nature of the adopted mathematical model.

The transition from the distributed load solution to the point load one is analysed numerically. As might be expected (see Figure 8), a distributed load smooths the singularities typical for a point load, e.g., those at Mach cones. We also mention that the effect of a distributed load is similar, in a sense, to that of an elastic coating [Erbaş et al. 2014].

A similar approach considered in this work may be readily extended to interfacial waves, e.g., Stoneley, Schölte, etc., and also to the media where the effects of prestress, layered structure and anisotropy are rather essential.

Acknowledgements

The authors would like to express their utmost gratitude to J. Kaplunov and D. A. Prikazchikov for fruitful discussions and insightful comments. This work is partly supported by the Research Projects of Anadolu University, Number 1306F268.

References

[Achenbach 1973] J. D. Achenbach, *Wave propagation in elastic solids*, Applied Mathematics and Mechanics **16**, North-Holland, Amsterdam, 1973.

[Achenbach 1998] J. D. Achenbach, "Explicit solutions for carrier waves supporting surface waves and plate waves", *Wave Motion* **28**:1 (1998), 89–97.

[Agostinacchio et al. 2013] M. Agostinacchio, D. Ciampa, M. Diomedi, and S. Olita, "Parametrical analysis of the railways dynamic response at high speed moving loads", *J. Mod. Transp.* **21**:3 (2013), 169–181.

[Cao et al. 2012] Y. Cao, H. Xia, and Z. Li, "A semi-analytical/FEM model for predicting ground vibrations induced by high-speed train through continuous girder bridge", *J. Mech. Sci. Technol.* **26**:8 (2012), 2485–2496.

[Celebi 2006] E. Celebi, "Three-dimensional modelling of train-track and sub-soil analysis for surface vibrations due to moving loads", *Appl. Math. Comput.* **179**:1 (2006), 209–230.

[Chadwick 1976] P. Chadwick, "Surface and interfacial waves of arbitrary form in isotropic elastic media", *J. Elasticity* **6**:1 (1976), 73–80.

[Courant and Hilbert 1962] R. Courant and D. Hilbert, *Methods of mathematical physics, II: Partial differential equations*, Wiley, New York, NY, 1962.

[Dieterman and Metrikine 1997] H. A. Dieterman and A. V. Metrikine, "Steady-state displacements of a beam on an elastic half-space due to a uniformly moving constant load", *Eur. J. Mech. A Solids* **16**:2 (1997), 295–306.

[El Kacimi et al. 2013] A. El Kacimi, P. K. Woodward, O. Laghrouche, and G. Medero, "Time domain 3D finite element modelling of train-induced vibration at high speed", *Comput. Struct.* **118** (2013), 66–73.

[Erbaş et al. 2013] B. Erbaş, J. D. Kaplunov, and D. A. Prikazchikov, "The Rayleigh wave field in mixed problems for a half-plane", *IMA J. Appl. Math.* **78**:5 (2013), 1078–1086.

[Erbaş et al. 2014] B. Erbaş, J. D. Kaplunov, D. A. Prikazchikov, and O. Şahin, "The near-resonant regimes of a moving load in a three-dimensional problem for a coated elastic half-space", *Math. Mech. Solids* (online publication October 2014).

[Galvín and Domínguez 2007] P. Galvín and J. Domínguez, "Analysis of ground motion due to moving surface loads induced by high-speed trains", *Eng. Anal. Bound. Elem.* **31**:11 (2007), 931–941.

[Gupta et al. 2010] S. Gupta, H. Van den Berghe, G. Lombaert, and G. Degrande, "Numerical modelling of vibrations from a Thalys high speed train in the Groene Hart tunnel", *Soil Dyn. Earthq. Eng.* **30**:3 (2010), 82–97.

[Kaplunov and Prikazchikov 2013] J. D. Kaplunov and D. A. Prikazchikov, "Explicit models for surface, interfacial and edge waves", pp. 73–114 in *Dynamic localization phenomena in elasticity, acoustics and electromagnetism*, edited by R. Craster and J. D. Kaplunov, International Centre for Mechanical Sciences Courses and Lectures **547**, Springer, Vienna, 2013.

[Kaplunov et al. 2006] J. D. Kaplunov, A. Zakharov, and D. A. Prikazchikov, "Explicit models for elastic and piezoelastic surface waves", *IMA J. Appl. Math.* **71**:5 (2006), 768–782.

[Kaplunov et al. 2010] J. D. Kaplunov, E. Nolde, and D. A. Prikazchikov, "A revisit to the moving load problem using an asymptotic model for the Rayleigh wave", *Wave Motion* **47**:7 (2010), 440–451.

[Kaplunov et al. 2013] J. D. Kaplunov, D. A. Prikazchikov, B. Erbaş, and O. Şahin, "On a 3D moving load problem for an elastic half space", *Wave Motion* **50**:8 (2013), 1229–1238.

[Kiselev and Parker 2010] A. P. Kiselev and D. F. Parker, "Omni-directional Rayleigh, Stoneley and Schölte waves with general time dependence", *Proc. R. Soc. Lond. A* **466**:2120 (2010), 2241–2258.

[Kiselev and Rogerson 2009] A. P. Kiselev and G. A. Rogerson, "Laterally dependent surface waves in an elastic medium with a general depth dependence", *Wave Motion* **46**:8 (2009), 539–547.

[Kiselev et al. 2007] A. P. Kiselev, E. Ducasse, M. Deschamps, and A. Darinskii, "Novel exact surface wave solutions for layered structures", *C. R. Mécanique* **335**:8 (2007), 419–422.

[Parker 2012] D. F. Parker, "Evanescent Schölte waves of arbitrary profile and direction", *Eur. J. Appl. Math.* **23**:2 (2012), 267–287.

[Parker 2013] D. F. Parker, "The Stroh formalism for elastic surface waves of general profile", *Proc. R. Soc. Lond. A* **469**:2160 (2013), Article ID #20130301.

[Poruchikov 1993] V. B. Poruchikov, *Methods of the classical theory of elastodynamics*, Springer, Berlin, 1993.

[Prikazchikov 2013] D. A. Prikazchikov, "Rayleigh waves of arbitrary profile in anisotropic media", *Mech. Res. Commun.* **50** (2013), 83–86.

[Rayleigh 1885] J. W. S. Rayleigh, "On waves propagated along the plane surface of an elastic solid", *Proc. Lond. Math. Soc.* **17** (1885), 4–11.

[Rousseau and Maugin 2011] M. Rousseau and G. A. Maugin, "Rayleigh surface waves and their canonically associated quasi-particles", *Proc. R. Soc. Lond. A* **467**:2126 (2011), 495–507.

[Zauderer 2006] E. Zauderer, *Partial differential equations of applied mathematics*, 3rd ed., Wiley, Hoboken, NJ, 2006.

Received 13 Jan 2016. Revised 13 Feb 2016. Accepted 9 Mar 2016.

BARIŞ ERBAŞ: berbas@anadolu.edu.tr
Department of Mathematics, Anadolu University, Yunusemre Campus, 26470 Eskişehir, Turkey

ONUR ŞAHIN: onur.sahin@anadolu.edu.tr
Department of Mathematics, Anadolu University, Yunusemre Campus, 26470 Eskişehir, Turkey

JOURNAL OF MECHANICS OF MATERIALS AND STRUCTURES

msp.org/jomms

Founded by Charles R. Steele and Marie-Louise Steele

Cover photo: Mando Gomez, www.mandolux.com

See msp.org/jomms for submission guidelines.

JoMMS (ISSN 1559-3959) at Mathematical Sciences Publishers, 798 Evans Hall #6840, c/o University of California, Berkeley, CA 94720-3840, is published in 10 issues a year. The subscription price for 2016 is US $575/year for the electronic version, and $735/year (+$60, if shipping outside the US) for print and electronic. Subscriptions, requests for back issues, and changes of address should be sent to MSP.

JoMMS peer-review and production is managed by EditFLOW® from Mathematical Sciences Publishers.

PUBLISHED BY

mathematical sciences publishers

nonprofit scientific publishing

http://msp.org/

Journal of Mechanics of Materials and Structures
Volume 11, No. 4 July 2016